Postprint of: Guzinski J., Abu-Rub H., Diguet M., Krzeminski Z., Lewicki A., Speed and Load Torque Observers Application in High-Speed Train Electric Drive, IEEE Transactions on Industrial Electronics, Vol. 57, Iss. 2 (2010), pp. 565-574, DOI: 10.1109/TIE.2009.2029582

Speed and Load Torque Observers Application in High Speed Train Electric Drive

Jaroslaw Guzinski, Haitham Abu-Rub, *Senior Member, IEEE*,
Marc Diguet, Zbigniew Krzeminski, Arkadiusz Lewicki,

***Abstract*— This paper present an application of induction motor mechanical speed and load torque observers in high speed train drives. The observers are applied for 1.2MW electric drive with induction motor. The goal of using such observers is to utilize computed variables for diagnostic purposes of speed sensors and torque transmission system. The concept of diagnostic system is presented in this paper and proper criteria are proposed. The suggested system is designed to work without speed sensor in the case of existing sensor faults. Monitored motor load torque is used to limit the maximum motor torque in case of existing problems in the gearbox. The results of simulation and experimental investigations for 1.2MW induction motor drive are presented.**

***Index Terms*— Observers, Diagnostics, Rail Vehicle, Induction motor, Sensorless control.**

I. Introduction

Diagnostic systems are presented in numerous papers [1]-[5], [7], and different techniques are being utilized for many important applications. One of the important applications is related to rail traction system [14].

The development of the rail transport is strongly dependent on the reliability of the rail vehicles. All of the rail systems should be equipped with appropriate diagnostic tools to assure a safe transport. Most of the diagnostic systems are equipped with additional sensors for safe operation. With extra sensors the vehicle becomes more complicated for maintenance. The new microprocessor techniques allow that the physical sensors can be replaced with the precise computational codes.

Typically, the traction motors are equipped with speed sensors. The sensor fault has significant influence on the proper working of the whole train system. Usually the rail vehicle is powered by few motors and few partially independent drives, while disconnecting anyone of the motors influences the train speed and consequently the travel time. In the traction drive, it is possible to use speed calculations instead of speed measurement [6]-[9], [29]. Using calculated speed, it is possible to e.g. switch to the speed sensorless system in case of speed sensor fault.

The motor torque transmission is the core system in traction drives. In the transmission system, the problems may appear even in new trains as a result of manufacturing or assembly errors e.g. misalignment of some parts of the transmission system [10]-[11]. After an initial period, the problems with the transmission may appear as a result of wearing and material consumption. Wear and tear of the gears causes growing amplitudes of the frequencies related to the gear meshing. To identify the problems related to the transmission system, typically an analysis of the motor or gear casing vibration, measured by the accelerometers, are done [12]-[13]. However, instead of the vibration measurement it is also possible to use the load torque calculation using observer systems [14]-[17].

For monitoring of both the electrical machines and transmission system, the load torque analysis is important [18]. For the load torque analysis it is difficult to unequivocally identify faults [19]-[21]. To define the torque transmission faults criteria it is essential to build initially a data base with load torque waveforms for healthy and faulty mechanical system, and then to define faults criteria.

In this paper an application of the motor speed and load torque observers is presented. The observers are proposed to be part of the diagnostic system for high speed train (HST) with 1.2 MW three-phase induction motor drive. Such application was previously presented in the authors' paper [22] and [23]. In [22] the used observers' structure was explained and the model of the mechanical system was presented. In [23] the concept of the diagnostic system based on observer systems was proposed. The appropriate diagnostic structures and criteria were suggested.

The proposed solution is a small part of the developed bigger HST predictive maintenance system. In the whole diagnostic system several problems are under consideration e.g.: speed sensor faults, mechanical transmission faults, motor stator and rotor faults etc.

In contrary to [22] and [23], the speed observer with exact model of the motor electromotive forces [28] is used in this paper. More detailed description of the experimental test procedure, additional test bench data and new simulation and experimental results are shown. The perspectives of future industrial implementation are discussed.

II. Description of the Rail and Test Bench Systems

The presented application of the speed and load torque observers is dedicated to the multiple unit high speed train which is shown in Fig. 1.

Manuscript received May 18, 2009. Accepted for publication July 20, 2009. This work was supported in part by the Ministry of Science and Higher Education under contracts N510 033 32/3050 and by finance for science in the years 2008–2010 as research project N N510 386735.

J. Guzinski is with Gdansk University of Technology, 80-233 Gdansk, Poland (corresponding author to provide phone: 4858-347-2960; fax: 4858-341-0880; e-mail: j.guzinski@ely.pg.gda.pl).

H. Abu-Rub is with Texas A&M University at Qatar, Doha, Qatar (e-mail: haitham.abu-rub@qatar.tamu.edu).

M. Diguet is with Alstom Transport, 65-000 Tarbes, France, (e-mail: marc.diguet@transport.alstom.com).

Z. Krzeminski and A. Lewicki are with Gdansk University of Technology, 80-952 Gdansk, Poland (e-mail: z.krzeminski@ely.pg.gda.pl; a.lewicki@ely.pg.gda.pl).

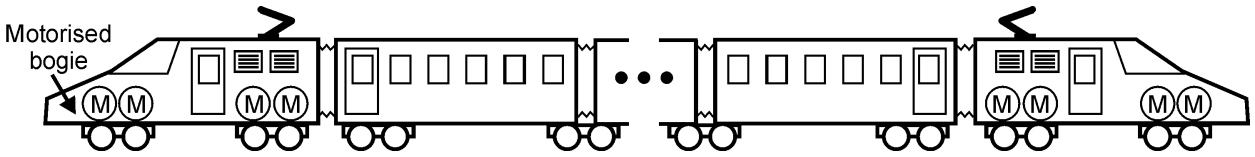

Fig. 1. Electric multiple unit with two power cars.

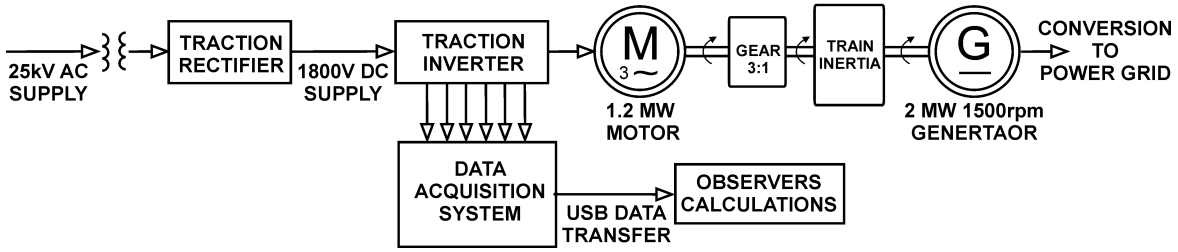

Fig. 3. High speed train (HST) test bench.

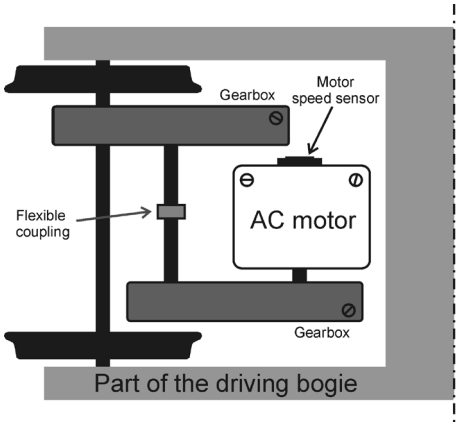

Fig. 2. Singular traction drive.

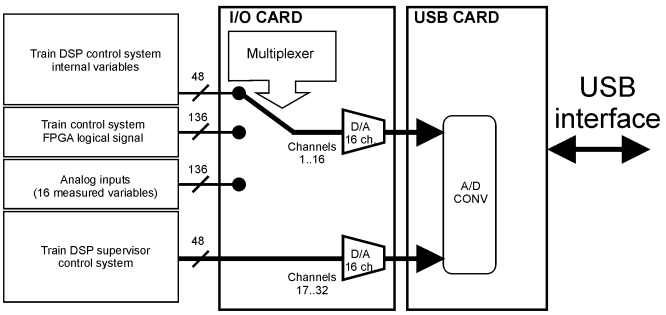

Fig. 4. Test bench data acquisition system (DAS).

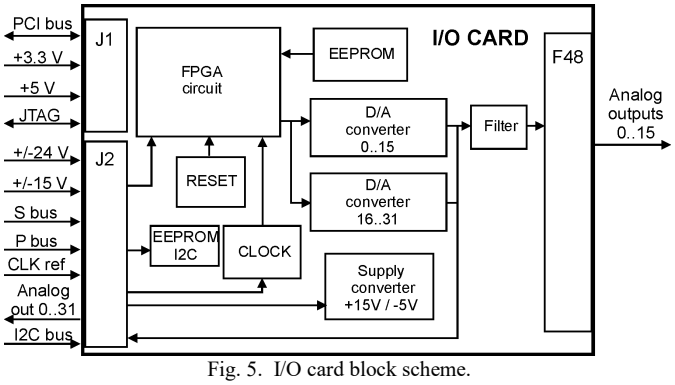

Fig. 5. I/O card block scheme.

In such considered system two power cars are used. Each car is propelled by four-1.2MW traction motors fed by separated converters. Each of the motors is coupled with separate axle with gear and coupling system. For the precise control of the motor each motor is supplied with different microprocessor controlled power converter (MCPC). In the train system all drives work under master control of the superior multiprocessor system (SMPS) which is an interface to the train operator and maintenance center.

Schematic diagram of the HST bogie transmission system was presented in [22] and [23]. More in detail is presented in Fig.2, where the two gears with Cardan flexible coupling are distinguished. For better shock absorption of the vehicle the heavy traction motors are fixed with car body. Therefore, the torque is transmitted from the motor to the wheels using two gears and flexible coupling. The total HST gear ratio is *1.9733*. The digital speed sensor is mounted directly on the motor shaft. Measured speed is used e.g. in the rotor flux observer calculations.

The experimental investigations of the observers presented in this paper were done in the train factory test bench (Fig. 3) where the traction motor, supply system and control were exactly the same as in the real motorized bogie. The structure of the gear was similar to the HST gear with different ratio. A special purpose data acquisition system (DAS) was used – Fig. 4.

The DAS is divided to the I/O card (IOC) – Fig. 5 and USB card (USBC). The IOC is communicating with the MCPC and SMPS using the internal buses. Configuration software is used to convert all of the MCPC and SMPS internal variables, as well FPGA logical signals, to the I/O card analog outputs. The train system sensors outputs are accessible in I/O system. Up to 32 analog signals are transferred from IOC to USBC and to the PC computer where data acquisition software is installed. The sampling for MCPC is 500μs for DSP variables, 10μs for FPGA signals and 20ms for SMPS variables and logical signals.

III. Model of the HST system and control principle

In the simulation model the next data of the real traction motor were used: 1.2 MW, 810 V, 280 rad/s, 397 rad/s. Motor speeds are related to the train speeds and are 225km/h and 320 km/h respectively. The parameters of the motor, which appear in simulation and experiments are normalized in per unit [6], [22], [23], [26], [28], [30].

The rotor field oriented control principle was used for motor control - Fig. 6. The mechanical part of the system was reduced to a two-mass system [22], [23]. Other data were presented in [22] and [23].

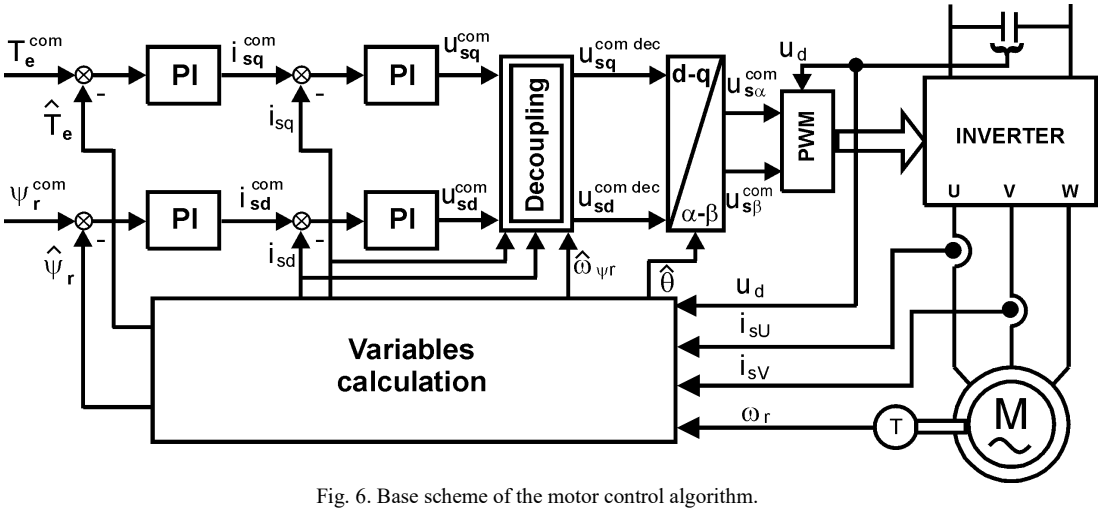

Fig. 6. Base scheme of the motor control algorithm.

IV. Traction Motor Speed Observer

A lot of speed observers were presented in the literature [29]. Extremely good results were obtained with the speed observer presented in [6]. The speed observer idea presented in [6] is based on extending the order of the Luenberger observer [27] with simple model of motor electromotive force (EMF):

$$\boldsymbol{\xi} = \omega_r \boldsymbol{\psi}_r \tag{1}$$

where $\boldsymbol{\xi} = \begin{bmatrix} \xi_\alpha & \xi_\beta \end{bmatrix}^T$, ω_r is motor mechanical speed, $\boldsymbol{\psi}_r$ is rotor flux: $\boldsymbol{\psi} = \begin{bmatrix} \psi_\alpha & \psi_\beta \end{bmatrix}^T$, and $\alpha\beta$ denote stationary frame of references.

When observer calculation period is small, is possible to assume that within one step the EMF are constant. Hence the additional state equation is used [6]:

$$d\xi / d\tau = 0 \tag{2}$$

where τ is time in per unit system.

In [6] the EMF is the observers disturbance which is estimated in pure integrators. In [30] the simplified dynamic equations for EMF disturbances were proposed and used for diagnostic purposes in [22] and [23]:

$$d\xi / d\tau = j\omega_r \xi \tag{3}$$

In this paper the newer version of the observer [28] was implemented. The newer version is based on EMF exact model:

$$d\xi / d\tau = a_5 \xi + a_6 \omega_r \mathbf{i}_s + j\omega_r \xi \tag{4}$$

where $a_5 = R_r / L_r$, $a_6 = R_r L_m / L_r$, and R_s, L_s, R_r, L_r, L_m are motor equivalent circuit parameters.

The equations of the speed observer are [28]:

$$d\hat{\mathbf{i}}_s / d\tau = a_1 \hat{\mathbf{i}}_s + a_2 \hat{\boldsymbol{\psi}}_r - j a_3 \hat{\xi} + a_4 \mathbf{u}_s^{com} + k_1 \left(\mathbf{i}_s - \hat{\mathbf{i}}_s \right) \tag{5}$$

$$d\boldsymbol{\psi}_r / d\tau = a_5 \boldsymbol{\psi}_r + a_6 \hat{\mathbf{i}}_s + j\hat{\xi} + \mathbf{e}_\psi \tag{6}$$

$$d\hat{\xi} / d\tau = a_5 \hat{\xi} + a_6 \omega_r \hat{\mathbf{i}}_s + j\omega_r \hat{\xi} + j k_4 \left(\mathbf{i}_s - \hat{\mathbf{i}}_s \right) \tag{7}$$

$$dS_{bF} / d\tau = k_{fo} \left(S_b - S_{bF} \right) \tag{8}$$

$$\mathbf{e}_\psi = \begin{bmatrix} -k_2 S_b \hat{\psi}_{r\alpha} + k_3 \hat{\psi}_{r\beta} \left(S_b - S_{bF} \right) \\ -k_2 S_b \hat{\psi}_{r\beta} - k_3 \hat{\psi}_{r\alpha} \left(S_b - S_{bF} \right) \end{bmatrix} \tag{9}$$

$$\hat{\omega}_r = \left(\hat{\xi}_\alpha \hat{\psi}_{r\alpha} + \hat{\xi}_\beta \hat{\psi}_{r\beta} \right) / \left(\hat{\psi}_{r\alpha}^2 + \hat{\psi}_{r\beta}^2 \right) \tag{10}$$

where: ^ denotes calculated value, $\mathbf{i}_s$, $\mathbf{u}_s^{com}$ are stator current and commanded stator voltages, S_b is observer stabilizing component, S_{bF} is S_b filtered value, $a_1 = -\left(R_s L_r^2 + R_r L_m^2 \right) / \left(L_r w_\sigma \right)$, $a_2 = R_r L_m / \left(L_r w_\sigma \right)$, $a_3 = L_m / w_\sigma$, $a_4 = L_r / w_\sigma$, $w_\sigma = L_r L_s - L_m^2$, k_1, k_2, k_3 and k_4 are observer gains, k_{fo} is S_b LPF coefficient.

In contrary to [28] the component related to $d\hat{\omega}_r / d\tau$ observer was omitted assuming that for small step of the observer calculation this component is close to zero in the high inertia train system The block and input/output scheme of the observer were presented in [22] and [23].

The speed observer is additionally used for motor electromagnetic torque calculations:

$$\hat{T}_e = \hat{\psi}_{r\alpha} \hat{i}_{s\beta} - \hat{\psi}_{r\beta} \hat{i}_{s\alpha} \tag{11}$$

V. Load Torque Observer (LTO)

For the diagnostic purposes the analysis of the motor load torque is used. This analysis was proposed in other papers but in most cases for the measured load torque [12]-[13]. Unfortunately, measurement of the load torque is complicated even in laboratory conditions and is rather practically inapplicable for industrial applications. According to the industry demand the computation method for the diagnostic purposes is used.

The load torque calculations are based on method presented in [7] and [14] and implemented for HST drive. Equations of the implemented load torque observer (LTO) are follows:

$$\frac{d}{dt} \begin{bmatrix} z_1 \\ z_2 \end{bmatrix} = \begin{bmatrix} 0 & -k_{1L} \\ 1 & -k_{2L} \end{bmatrix} \begin{bmatrix} z_1 \\ z_2 \end{bmatrix} + \begin{bmatrix} k_{1L} b J_M \\ \left(k_{2L}^2 - k_{1L} \right) J_M \end{bmatrix} \hat{\omega}_r + \begin{bmatrix} k_{1L} \\ k_{2L} \end{bmatrix} \hat{T}_e \tag{12}$$

$$\hat{T}_{S1} = z_2 - k_{2L} J_M \hat{\omega}_r \tag{13}$$

where: k_{1L}, k_{2L} are LTO gains, z_1, z_2 are LTO internal state variables and $\hat{T}_e$ is motor torque calculated by speed observer.

In the LTO equations the estimated motor speed is used. It makes LTO system independent of speed sensors faults. In the real HST system the accuracy of the LTO calculations is better with calculated speed than with measured one. This is a result of low resolution of the motor speed sensor used in the real HST and in the test bench. This speed sensor accuracy is 6% and 240 pulses per revolution. This low resolution of the

sensor is the result of long term continuation of the HST technology.

VI. Observers verification procedures

Both observers were investigated by simulation and experimentally for 1.2 MW HST drive.

For simulation the system was implemented in C language with help of Matlab/Simulink as separate S-function.

For the experimental verification the train factory test bench was used. Due to limited access a two-step procedure was used in the experiments. In the first step the list of desired tests was prepared and required MCPC variables and measurements were collected with help of DAS: input inverter voltage, motor speed, PWM modulation index, angle position of PWM commanded voltage vector and motor two phase currents.

The tests were done on the test bench: start up of the train and work with constant speed with different load levels and motor speed, breaking of the train with different load levels and work with different constant motor speed for 0%, 25%, 50%, 75% and 100% load etc.

The collected signals were sampled with the same frequency as MCPC calculation frequency 2kHz. Recorded waveforms were saved by the PC connected to DAS and converted into Matlab files format. An example of waveform is in Fig. 7.

For experimental records the observer procedures calculation were done off-line in PC with Matlab. The experimental data were used as inputs for observers S-function. The off-line observers' calculations were done with different sampling frequencies: 2kHz, 5kHz, 10kHz and 20kHz. Good results were obtained for 20kHz. The difference between 2kHz MCPC and observer calculation sampling is resulted from the fact that MCPC and observers' calculations were not been synchronized with the inverter PWM and the sensors sampling. On the base of the performed simulations is predicted that in case of observers procedures implementation in the MCPC both MCPC and observer calculations sampling frequencies will be the same.

The correctness of the S-function observers C language code was verified in the designed SH65L type DSP board with ADSP21065L fixed point processor and FPGA. The real system with the observers and DSP board as well converter and an induction motor drive were tested in the small scale 1.5kW laboratory setup.

VII. Speed Observer Investigations

Simulation results for the speed observer from section IV are presented in Fig. 8.

In Fig. 8 the motor load torque was changed in steps. Adequately to the commanded torque the speed of the motor changes. The particular steady state motor speeds are related to the speed of the train: 30..160..210..150km/h. During the test the speed observer was working properly. In comparison to other observers accuracy [29] the motor speed calculation error was small – up to 1.3% of the motor nominal speed in full speed range. It is also better than results obtained with previous version of the traction motor speed observer [22], [23]. The accuracy of the calculated motor speed is better than the accuracy of the measured speed used in HST (6%) so it is evident that estimated speed could be used as useful tool for the diagnostic system.

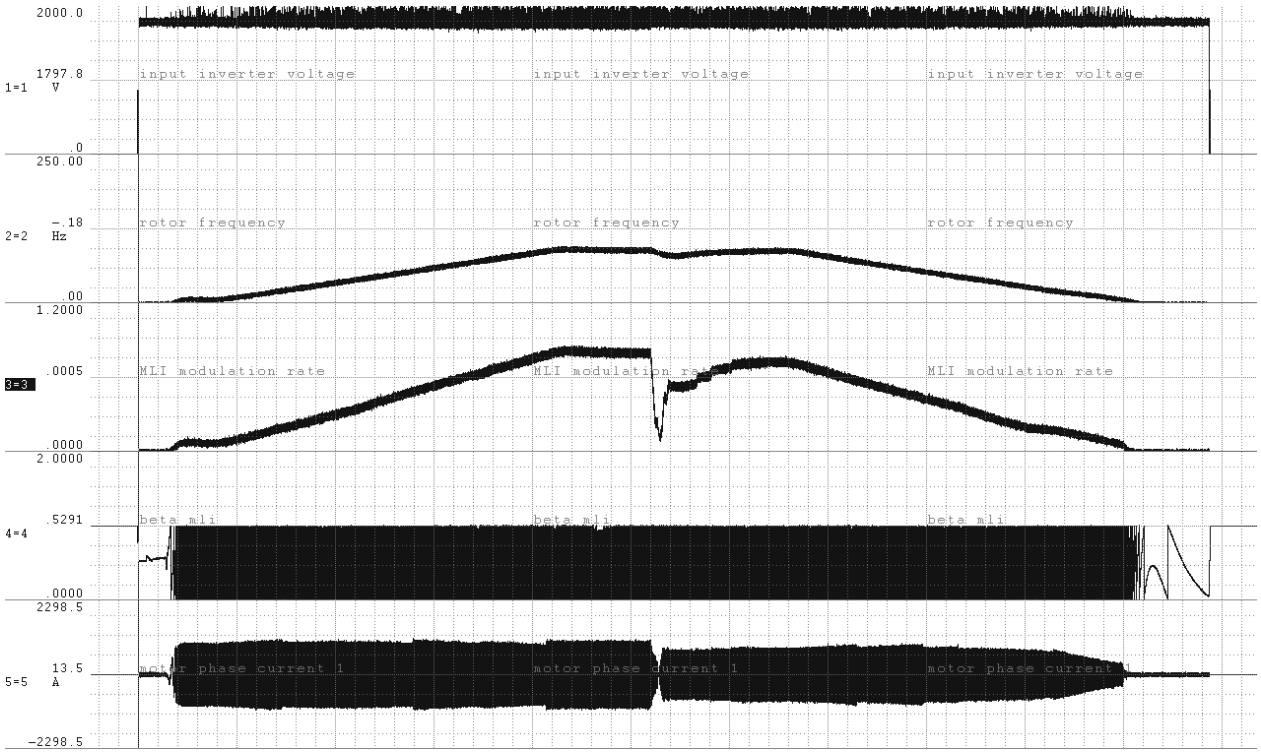

Fig. 7. Experiment: the example of the recorded waveforms during motor start up – visible motor maximum speed corresponds to 100 km/h speed of the train (1-inverter supply voltage, 2-motor speed, 3-PWM modulation index, 4-motor supply voltage vector position, 5 - stator currents,).

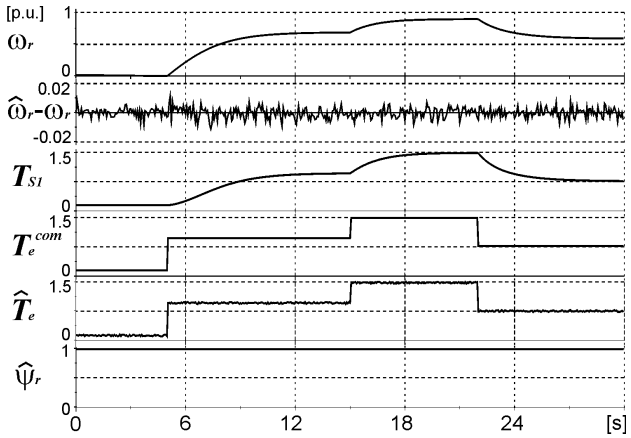

Fig. 8. Simulation results for speed observer during accelerating and decelerating of the train (30..160..210..150 km/h).

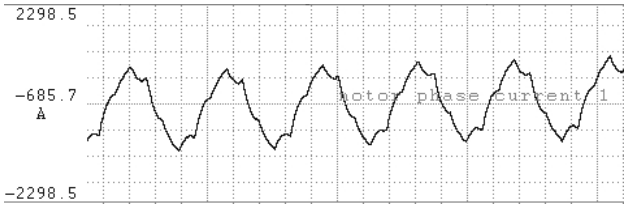

Fig. 9. Motor current for the 320km/h train speed and 100% load

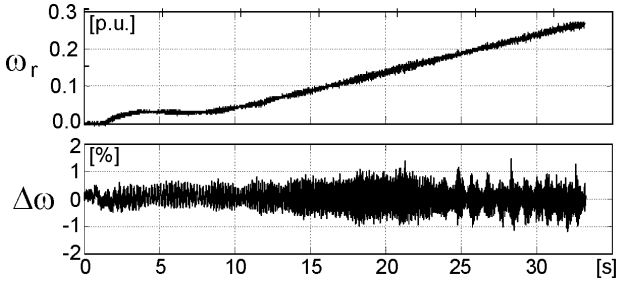

Fig. 10. Experimental results for speed observer calculation – start up of the train from 0 km/h to about 50 km/h

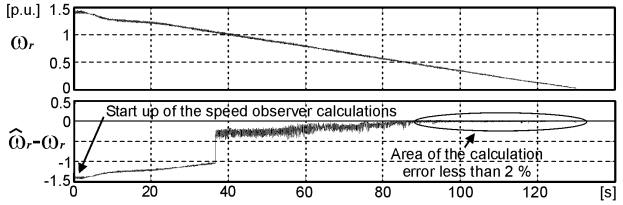

Fig. 11. Experimental results for speed observer calculation – breaking of the train from 320 km/h to 0 km/h – observer calculation starts when the train has the higher speed

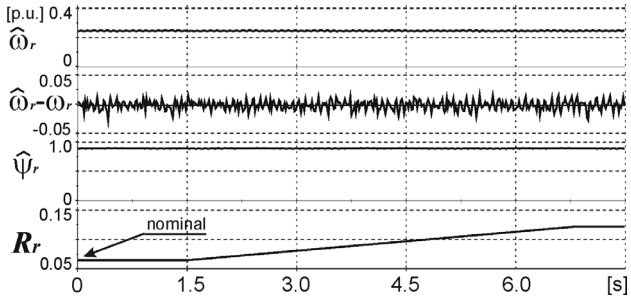

Fig. 12. Small scale (1.5kW) experimental result –system reaction to the changes of the motor rotor resistance.

In [22] the experimental test of the speed observer in the whole train speed range was presented. In spite of changing the inverter transistors switching frequency the observer was working properly even for the highest obtained speed. In the upper speed range the inverter was working with square wave and the motor current shape was strongly deformed – Fig. 9. Experimental results for the new version of the observer is presented in Fig. 10.

In Fig. 10 the train drive was started to about 50 km/h. The speed observer is working with an error less than 1.5 %, which is similar to the simulation results. In contrary to results from [23] the error is significantly lower for the low speed region.

If the observer calculations start when the inverter switching frequency is high and the motor current are close to sinusoidal shape, the observer acts properly. In case when the observer calculations are switched on when the train is working with higher speed and the current is deformed, the observer can not start – Fig. 11.

In Fig. 11 the observer started to work properly when the speed of the motor has decreased to the level responding about 120 km/h. With this speed level the current quality has improved and becomes suitable for the speed observer.

The reaction to the motor parameters' changes were tested experimentally in a 1.5kW induction motor drive. The variations of the motor parameters were been applied in the observer equations. An example is in Fig. 12. In spite of wide rotor resistance deviation, the system keeps stability. The commanded speed (0.32 p.u.) and flux (0.9 p.u.) are controlled. The use of the closed loop observer structure makes the system practically non sensitive to the parameters variations.

VIII. Speed Sensor Diagnostic System Idea

The speed observer was proposed to be used as an element of the speed sensor diagnostic system. The diagnostic idea was tested by simulation method.

With on-line speed calculation it is possible to compare the measured speed with the calculated one. It is obvious that a practically applicable diagnostic criterion for speed sensors could be:

$$\left|\hat{\omega}_r - \omega_r\right| > E_{r\,limit} \tag{20}$$

where the error limit $E_{r\ limit}$ was tuned to the level $E_{r\ limit}$=3%. This level was chosen to be higher than the maximum speed error calculations obtained in simulation and the indicator level should be tuned according to the obtained speed observer accuracy.

If the $E_{r\ limit}$ exceeds tuned diagnostic level the SMPS obtains the adequate diagnostic information. In case of speed sensor fault detection it is desirable to switch the motor control to the speed sensorless mode. Additionally, the diagnostic information should be sent to the maintenance center through rail wireless communication interface [23].

IX. Speed Sensorless Control of the Drive

The measured speed of the motor is converted in the control board and sent to the microprocessor system. If the fault of the speed sensor occurs, this information can be disturbed in different ways – depending on the realization of the MCPC digital input buffer. In the faulty case the scanned motor speed

can change rapidly to some of the buffer limits. It is possible also that scanned speed can stay without changes – if input buffer will memorize the last correct value. Depending on the type of the fault the control system may react differently.

The HST system was tested in simulation program for some cases of the speed sensors faults. An example results are presented in Fig. 13.

In Fig. 13 the speed sensor fault appears at instant 5 sec. At this instant the measured speed was equated to zero. In one step of the control system calculation that fault was detected and a diagnostic indicator $d_{\omega r}$ has been changed from 0 to 1. Simultaneously, the system was switched to the speed sensorless mode. The whole system works without any disturbance. After fault the commanded motor torque was changed and the system has reacted correctly.

The other fault of the speed sensor is also probable – in the speed scanning buffer the last proper value of the measured speed could be memorized. If this happens during a steady state the diagnostic system does not react immediately. In such case the whole system still works properly until the moment when the torque commanded signal is set or when the system starts losing its operating point. An example of such incident is in Fig. 14.

In Fig. 14 the speed sensor fault has appeared at instant 5sec. In the speed scanning buffer the last proper value was memorized. The whole control system was in steady state condition and the fault was not identified. That fault has no influence on the system work until the moment when the system started to change the actual operating point slowly. When the diagnostic indicator achieved 3% level, the fault was indicated and control was switched to the sensorless mode.

For sensorless control of the drive the difference between the speed observers from [22], [23] and speed observer presented in this paper are not noticeable. As was presented in e.g. [29] the sensorless control drives can work also with the higher speed errors. Practically the speed estimation error level can influence significantly on the proper work of the drive only in the very low speed range. The quality of the speed observer has more significant importance for the diagnostic purposes.

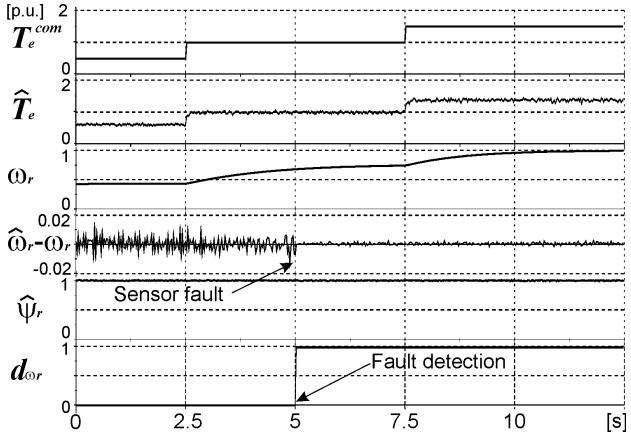

Fig. 13. Control of the HST drive with diagnostic system during speed sensor faults - zero speed in the control system memory.

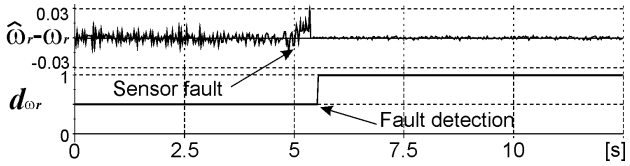

Fig. 14. Detection of the sensor faults – last measured speed value in the control system memory.

It is assumed that to discern between the sensor failure and motor failure a different motor stator and rotor diagnostic system has to be used. The HST motor failure is going to be monitored by separate algorithm based on analysis of the control signals in the closed loop [31].

X. Load Torque Observer Investigations

Presented LTO was verified with simulation and experiments in the same way as the speed observer.

An example of the LTO simulation result is presented in Fig. 15. The experimental results are in Fig 16 and 17.

For Fig. 15 the inertia of the train was omitted and the superior motor speed controller was used. The mechanical part of the simulated system was not faulty. The load torque T_L was applied with step changes for different motor speeds. The estimated motor load torque $\hat{T}_{S1}$ follows the real motor load torque T_{S1}. Other results of the LTO were presented in [22], [23].

In Fig. 16 and Fig. 17 the train was moving with constant speed of 50 km/h and 150 km/h respectively. The four different motor loads: 25 %, 50 %, 75 %, 100 % were applied. The calculated load torque was analyzed with discrete Fourier transformation. In the shown figures only some interesting range of frequency is presented. This frequency range was related to the load torque meshing frequency. The train speed 50 km/h is equal to 29 Hz frequency of the motor rotation speed and the 150km/h to 90Hz respectively. The mechanical speed of the motor comes from the used gear ratio (1.97), wheel diameter (0.885 m) and the motor poles number (6) [22]. Regarding the teeth number of the gear driving wheel - 25, the meshing frequency was approximately 725 Hz and 2250 respectively. In the test bench the transmission system was healthy and the amplitude of the meshing frequency was very small but was identified using the proposed calculation method. In the case of the 150km/h train speed the motor speed was calculated with less accuracy. So the motor mechanical speed was variable in the range 87 to 90Hz. It influences on the results presented in Fig. 17.

Other tests were provided for higher train speed but for a reason of lower switching frequency of the inverter transistors the motor current was seriously distorted [22]. Therefore, for higher speed the LTO results were not satisfying. That is partially visible even in Fig. 17 waveforms where meshing frequency amplitudes are close to other visible in load torque spectrum.

In the real system the diagnostic system for gear monitoring will not work in all range of the HST speed. The suggested range of the HST speed, accessible for LTO calculations, is up to 100 km/h.

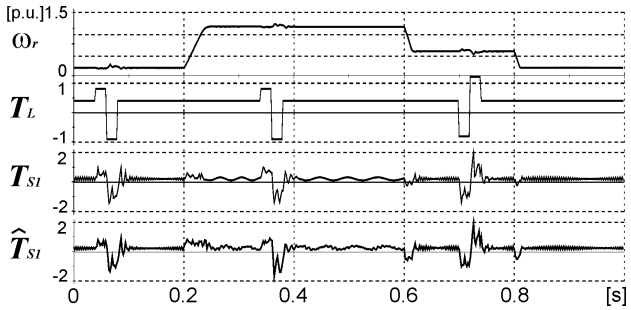

Fig. 15. Simulation results for LTO calculation.

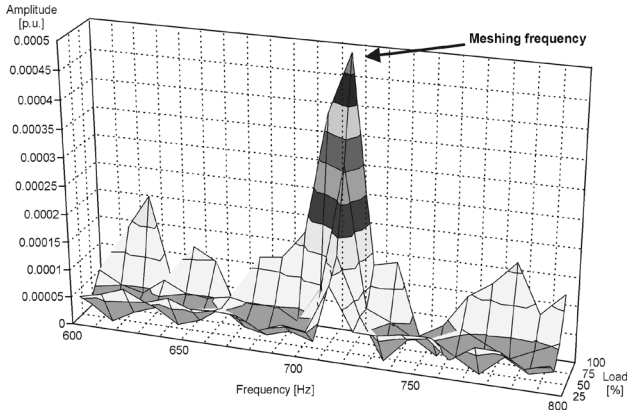

Fig. 16. Experimental results for load torque observer calculation – identification of meshing frequency – train speed about 50 km/h.

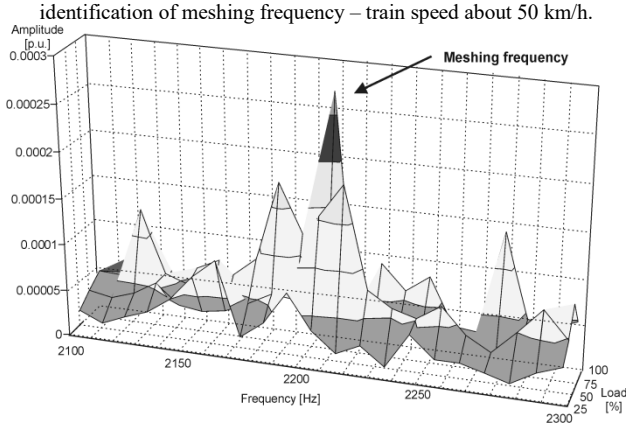

Fig. 17. Experimental results for load torque observer calculation – identification of meshing frequency – train speed about 150 km/h.

XI. Torque Transmission Diagnostic System Idea

The idea of the torque transmission monitoring system depends on the assumption that all the problems within the transmission system could be identified by the motor load torque analysis. In the diagnostic system the load torque of the motor will be calculated using the motor load torque observer. As reported in numerous papers, the analysis of the load torque is very complicated. Therefore, the analysis of the motor load torque should be divided into two methods: on-line and off-line [22], [23].

In on-line method a simple comparison of the amplitudes of the characteristic frequencies should be used to identify the serious problems with the transmission system. When a problem is identified the control system should limit the maximum torque generated by the motor to allow slower travel of the train. For predicting some symptoms of the mechanical system faults a more complicated and time consuming procedures will be essential e.g. detectors based on fuzzy logic and neural networks.

XII. Implementations Perspectives and Conclusions

The obtained results confirm that the speed and load torque observers has good properties to be used in the diagnostic system. The proposed solution was accepted by HST factory for future implementation and for consecutive tests. Currently, our diagnostic system is under implementation in the real rail system as an open-loop system. The separate DSP diagnostic board (DSPDB) is under development and is planned to be installed it in the real running HST. In the first step the DSPDB will work in open-loop calculating. The observers will be used for data collecting purposes and monitoring. The data will be stored in the DSPDB flash memory and transmitted to the maintenance center. These data will be analyzed and compared with the other data kept in the maintenance center records. This solution is necessary for building a torque transmission system failures data base, which will be used to define diagnostic criteria and their appropriate excitation levels. After that it is planned to include the DSPDB to the closed-loop control of the HST. The DSPDB will communicate with SMPS sending information about appearing or predicted faults.

Acknowledgements

The authors thank Mr. Jean-Marc Descures from Alstom Transport, Tarbes, France for his help with preparing the experimental tests.

References

[1] J. F. Martins, V. F. Pires, A. J. Pires, Member, "Unsupervised neural-network-based algorithm for an on-line diagnosis of three-phase induction motor stator fault", *IEEE Trans on. Industrial Electronics, v*ol. 54, no. 1, pp. 259 – 263, February 2007.

[2] S. H. Kia, H. Henao, G. A. Capolino, "A high-resolution frequency estimation method for three-phase induction machine fault detection" ", *IEEE Trans on. Industrial Electronics, v*ol. 54, no. 4, pp. 2305 – 2314, August 2007.

[3] S. Khomfoi, L. M. Tolbert, "Fault diagnosis and reconfiguration for multilevel inverter drive using AI-based techniques", *IEEE Trans on. Industrial Electronics, v*ol. 54, no. 64, pp. 2954 – 2968, December 2007.

[4] Y. M. Chen, H. C. Wu, M. W. Chou, K. Y. Lee, " Online failure prediction of the electrolytic capacitor for LC filter of switching-mode power converters", *IEEE Trans on. Industrial Electronics, v*ol. 55, no. 1, pp. 400 – 406, January 2008.

[5] S. Y. Kim, K. Nam, H.-S. Song, H.-G. Kim, " Fault diagnosis of a ZVS DC–DC converter based on DC-link current pulse shapes", *IEEE Trans on. Industrial Electronics, v*ol. 55, no. 3, pp. 1491 – 1494, March 2008.

[6] Z. Krzemiński, "Sensorless control of the induction motor based on new observer", in Proc. *International Conference on Power Electronics, Intelligent Motions and Power Quality, PCIM 2000*, Nuremberg, Germany, 2000.

[7] K. Ohnishi, M. Shibata, T. Murakami, "Motion control for advanced mechatronics", *IEEE/ASME Transactions on Mechatronics*, vol. 1, no. 1, pp. 56-67, 1996.

[8] L. Harnefors, M. Hinkkanen, " Complete stability of reduced-order and full-order observers for sensorless IM drives"", *IEEE Transactions on Industrial Electronics*, vol. 55, no. 31, pp. 1319-1329, March 2008.

[9] D. Traoré, F. Plestan, A. Glumineau, J. Leon, "Sensorless induction motor: high-order sliding-mode controller and adaptive interconnected observer", *IEEE Transactions on Industrial Electronics*, vol. 55, no. 11, pp. 3818-3827, November 2008.

[10] K.M. Al-Hussain, "Dynamic stability of two rigid rotors connected by a flexible coupling with angular misalignment", *Journal of Sound and Vibration*, no. 266, pp.217–234, 2003.
[11] N. Driot, J. Perret-Liaudet, "Variability of modal behavior in terms of critical speeds of a gear pair due to manufacturing errors and shaft misalignments", *Journal of Sound and Vibration*, no. 292, pp.824–843, 2006.
[12] A. C. J. Luo, "Past, current and future on nonlinear dynamics and noise origins of non-smooth gear transmission dynamic systems", in Proc. *IEEE*, 2005, pp. 674-681.
[13] L. Vedmar, A. Andersson, "A method to determine dynamic loads on spur gear teeth and on bearings", *Journal of Sound and Vibration*. no. 267, pp.1065–1084, 2003.
[14] S. Kadowaki, K. Ohishi, T. Hata, N. Iida, M. Takagi, T. Sano, and S. Yasukawa, "Antislip readhesion control based on speed-sensorless vector control and disturbance observer for electric commuter train—series 205-5000 of the East Japan Railway Company", *IEEE Transactions on Industrial Electronics*, vol. 24, no. 4, pp. 2001-2007, August, 2007.
[15] A. Hace, K. Jezernik, A. Šabanovic, "SMC with disturbance observer for a linear belt drive", *IEEE Transactions on Industrial Electronics*, vol. 54, no. 6, pp. 3402-3412, December 2007.
[16] K. Szabat, T. Orlowska-Kowalska, " Performance Improvement of Industrial Drives With Mechanical Elasticity Using Nonlinear Adaptive Kalman Filter", *IEEE Transactions on Industrial Electronics*, vol. 55, no. 3, pp. 1075-1084, March 2008.
[17] D. Brambilla, L. M. Capisani, A. Ferrara, P. Pisu, "Fault detection for robot manipulators via second-order sliding modes", ", *IEEE Transactions on Industrial Electronics*, vol. 55, no. 11, pp. 3954-3963, November 2008
[18] M. Blödt, P. Granjon, B. Raison, G. Rostaing, "Models for bearing damage detection in induction motors using stator current monitoring", *IEEE Trans on. Industrial Electronics, v*ol. 55, no. 4, pp. 1813 – 1822, April 2008.
[19] C. D. Begg, T. Merdes, C. Byington, K. Maynard, "Dynamics modelling for mechanical fault diagnostics and prognostics", in Proc. Mechanical System Modeling for Failure Diagnosis and Prognosis, Maintenance and Reliability Conference, MARCON'99, Gatlinburg, Tennessee, 1999, pp. no numbered.
[20] S. Silva, M. Dias Jr., "Statistical damage detection in stationary rotor systems through time series analysis", in Proc. Brazilian Conference on Dynamics, Control and Their Applications, DINCON 2006, Guaratinguetá, Brazil, 2006, pp. no numbered.
[21] A. M. Silva, R. J. Povinelli, N. A. O. Demerdash, "Induction machine broken bar and stator short-circuit fault diagnostics based on three-phase stator current envelopes", *IEEE Trans. on Industrial Electronics, v*ol. 55, no. 3, pp. 1310 – 1318, March 2008.
[22] J. Guzinski, M. Diguet, Z. Krzeminski, A. Lewicki, H. Abu-Rub., "Application of Speed and Load Torque Observers in High Speed Train Drive for Diagnostic Purposes", *IEEE Trans. on Industrial Electronics,* vol. 56, no. 1, pp. 248–256, January 2009.
[23] J. Guzinski, M. Diguet, Z. Krzeminski, A. Lewicki, H. Abu-Rub., "Application of Speed and Load Torque Observers in High Speed Train", in Proc. *13th International Power Elecronics and Motion Control Conference EPE-PEMC 2008,* Poznan, Poland, 2008, pp. 1405-1412.
[24] S. Villwock, M. Pacas, "Application of the welch-method for the identification of two- and three-mass-systems", *IEEE Trans on. Industrial Electronics, v*ol. 55, no. 1, pp. 457 – 466, January 2008.
[25] M. S. Tondos, "Minimizing electromechanical oscillations in the drives with resilient couplings by means of state and disturbance observers" , in Proc. *European Power Electronics Conference, EPE1993*, Brighton, UK, 1993, pp. 360–365.
[26] M. Wlas, Z. Krzeminski, H. A. Toliyat, "Neural-Network-Based Parameter Estimations of Induction Motors", *IEEE Trans on. Industrial Electronics, v*ol. 55, no. 4, pp. 1783 – 1793, April 2008.
[27] D. G. Luenberger, "An introduction to observers", *IEEE Transactions on Automatic Control*, vol. AC-16, no. 2, pp. 596-602, 1971.
[28] Z. Krzemiński, "Observer of induction motor speed based on exact disturbance model", in Proc. Int. Conf. EPE-PEMC 2008, Poznan, Poland, 2008, pp. 2325-2330.
[29] K. Rajashekara, A. Kawamura, K. Matsuse, "Sensorless Control of AC Motor Drives", IEEE Industrial Electronics Society, IEEE Press, 1996.
[30] M. Adamowicz, J. Guziński, "Control of Sensorless Electric Drive with Inverter Output Filter", in Proc. 4th Int. Symposium on Automatic Control AUTSYM 2005, Wismar, Germany, 22-23 September 2005, pp. not numbered.
[31] S. M. A. Cruz, A. J. M. Cardoso, "Diagnosis of Rotor Faults in Closed-Loop Induction Motor Drives", in Proc. IEEE/ IAS Annual Meeting. Conference, Tampa Florida, USA, 8-12 October 2006, pp.: 2346-2353.

Jaroslaw Guzinski received the M.Sc. and Ph.D. degrees from the Electrical Engineering Department at the Technical University of Gdansk, Poland, in 1994 and 2000, respectively. Currently he is an Adjunct with the Faculty of Electrical and Control Engineering at Gdansk University of Technology, Poland. His current interests include sensorless control of electrical motors, digital signal processors and electric vehicles.

Haitham Abu-Rub (M'99-SM'07) received Ph.D. degree in 1995 from Electrical Engineering Department at the Technical University of Gdansk in Poland. Since 1997 he has been with Birzeit University in Palestine. Currently, he is the Chairman of Electrical Engineering Department and holds the position of associate professor. His main research interests include electric motor drives, power electronics, and electrical machines.

Marc Diguet was born in 1956. Graduated from the Ecole Nationale d'Electronique et de Radio-Electricite de Grenoble (INPG), Grenoble, France. Since 1985 within Alstom Transport, Tarbes, France. Technical project manager for Electrical Multiple Units projects for SNCF, RATP (French transport operators) and SJ (Swedish transport operator). Joined the traction products Alstom Research and Development department since 2006.

Zbigniew Krzeminski received the Ph.D. degree from the Technical University of Lodz, Poland in 1983, and the D.Sc. degree from Silesian Technical University, Gliwice, Poland, in 1991. Currently, he is a Professor with the Gdansk University of Technology, Poland. His main areas of research are modeling and simulation of electric machines, control of electric drives, and DSP systems.

Arkadiusz Lewicki received the received the M.Sc. and Ph.D. degree in electrical drives specialization from Faculty of Electrical Engineering, Gdansk University of Technology, Gdansk, Poland in 1998 and 2003 respectively. He works at The Institute of Automatic Control of Electric Drives in Gdansk University of Technology. His scientific activities are concentrated on microprocessor control of converters, PWM techniques and nonlinear control.